INVESTIGATION OF CLOUD PROPERTIES AND ATMOSPHERIC PROFILES WITH MODIS

SEMI-ANNUAL REPORT FOR JAN-JUN 1998

Paul Menzel, Steve Ackerman, Chris Moeller, Liam Gumley, Kathy Strabala,
Richard Frey, Elaine Prins, Dan LaPorte and Walter Wolf
CIMSS at the University of Wisconsin
Contract NAS5-31367

ABSTRACT

The delivery of the MODIS version 2 production software packages has allowed the UW group to concentrate on fine tuning MODIS production algorithms and publishing results. Confidence in the quality of the MODIS cloud retrieval algorithms continues to grow as they are applied to more challenging MAS scenes and as validation data becomes available. A significant effort is underway to prepare our SCF for at launch MODIS processing. This includes the installation and testing of newly arrived SGI hardware and porting of DAAC approved software. UW personnel continue to work with MAST in the AM-1 infrared characterization of MODIS.

TASK OBJECTIVES

Software Development

Delivery of the UW science production software packages (cloud mask, cloud top properties, cloud phase, atmospheric profiles, and ancillary data) were completed in fourth quarter 1997. Further integration of the software into the DAAC processing environment involves periodic dialogue and collaboration between SDST personnel and UW. Rigorous testing of the algorithms using MAS data as a MODIS surrogate is underway; resulting additions and improvements are expected to be integrated prior to launch

MODIS Infrared Calibration

Chris Moeller and Dan LaPorte continue to participate in MODIS IR calibration activities. Both attended the MODIS Infrared Calibration Workshop in Miami in February and the MODIS Characterization Workshop held at GSFC on 23 June. At these workshops, MCST reported on AM-1 calibration progress and plans for FM-1 testing. The UW also delivered regression coefficients to the MCST relating MODIS 7.34 micron (band 28) radiance and the 5.3 micron SWIR leak radiance, which were simulated using radiosondes and a forward model.

Atmosphere Group Meeting

Four members of the UW MODIS team attended the Atmosphere Group Retreat at St. Michael's Maryland on 3-5 February. The meeting was productive in reconnecting the group on science issues that had taken a back seat to software delivery requirements.

WORK ACCOMPLISHED

MODIS Software Development

Although the UW MODIS Version 2 software packages were delivered in fourth quarter 1997, several software iterations between SDST and UW personnel were necessary before the MODIS Version 2 code was baselined. Most of the iterations involved refinements to the ancillary data subroutine to accommodate PGS requirements.

Several additions and improvements to the Version 2 software are underway. It is anticipated that these changes will be included in the at launch Version 2 code.

1) Addition of clear radiance maps to both the cloud mask and cloud top properties packages. Walter Wolf has set up a system to create the clear radiance data files for use in the Cloud Mask code (MOD_PR35). When each granule is processed in the MOD_PR35 code, a temporary clear radiance map file will be created. The pixels determined to be clear by the cloud mask are used to create this temporary clear radiance map file. These temporary files will have a resolution of 0.25 degrees in both latitude and longitude around the globe (producing 1036800 pixels). To save disk space on the operating computer, these temporary files are pseudo compressed. Each of the files will have a unique name determined by the time and date of the data along with the granule's position on the globe. At the end of the day, a program will be run to take all the temporary files and produce a global daily composite along with an updated eight day composite. The composite clear radiance files will be archived in HDF format. The method used in the Version 1 code was rejected due to size, time and processing constraints. Numerous work arounds were attempted prior to Version 2 delivery, but none satisfied all SDST and DAAC requirements.

2) Addition of a high resolution near real-time global snow base map, produced by the National Snow and Ice Data Center (NSIDC) for use by EOS investigators. This data set is being tested in the daily AVHRR LAC cloud mask processing, and will be used in MODIS product generation until the cloud mask and MODIS snow mask products become stable.

3) Day/night separation of cloud top property parameters necessary for atmosphere group science investigations. Some of the atmosphere group products are produced using data from day time only. Science investigations which compare aggregated Level 3 gridded products produced from both day and night data with those produced from day only data may yield biased results.

4) Addition of the global 1 km ecosystem base map distributed by the Earth Resources Observations Systems (EROS) Data Center Distributed Active Archive Center (EDC DAAC). We are currently using a 10 minute global base map and a 1 km map over North America only.

Walter Wolf continues to work with SDST to create the atmosphere group level 3 (MOD08) output HDF product file. This work includes making modifications to the CDL file specification and to the existing C code, which reads in the file specification and creates an output FORTRAN subroutine containing all the information from the CDL file. This output FORTRAN subroutine is then used by SDST software to create the output level 3 HDF file automatically.

Comparison of MODIS Radiance to Brightness Temperature Techniques

Walter Wolf also performed a comparison of the results of the radiance to brightness temperature conversion techniques used by each MODIS group. Unfavorable comparisons may bias cross-discipline studies. Planck functions that the ocean (FORTRAN 90), land (C Code) and atmosphere (FORTRAN 77) groups are using were downloaded and compiled. A test was performed by passing in a radiance value into all algorithms for MODIS bands 20, 29, 31 and 33 and the derived brightness temperatures were compared. The results for each band are described below:

Band 20 (3.7 μm): The difference between the land and ocean brightness temperature calculations was less that 0.1 K when applied to a radiance interval of 0.1 to 1 W/m2/ster/μm, whereas, the difference between the atmosphere and land (or ocean) was very large, approaching 2 degrees.

Band 29 (8.6 μm): A radiance interval of 5.0 to 14.0 W/m2/ster/μm was used to calculate the brightness temperatures. The difference between all group calculations was less than 0.04 K.

Band 31 (11 μm): A radiance interval of 6.0 to 14.0 W/m2/ster/μm was used to calculate the brightness temperatures. The difference between the land and ocean calculations was less than 0.03 K, between atmosphere and land values less than 0.05 K, and between the atmosphere and ocean less than 0.08 K for all input radiances.

Band 33 (13.3 μm): A radiance interval of 5.0 to 11.0 6.0 to 14.0 W/m2/ster/μm was used to calculate the brightness temperatures. The difference in the results between all three groups was less than 0.025 K.

Liam Gumley presented these results at the MODIS Science Team Meeting on 25 June. An action item was assigned to Bob Murphy to coordinate a MODIS approach for radiance to brightness temperature conversions.

Visualization Software

In the first quarter of 1998, that MODIS group began producing cloud height and phase products from MAS HDF data for the first time. Since this processing was carried out entirely outside the McIDAS environment, new visualization tools were needed to display

the results along with the image data. For this purpose, a new procedure was developed in IDL which permits the display of individual MAS bands, along with graphics overlays of the cloud mask, cloud height, or cloud phase results. Graphical output from this procedure was presented at the MODIS Atmosphere Group Retreat, February 3-5, St. Michaels, MD.

A new version of the MAS visualization program SHARP was released on the Web on May 5. The new version included the following updated features:

- User selectable image units (reflectance/temperature or radiance),
- Continuous display of data values (Pixel, Scanline, Time, Lat, Lon, Value) under cursor,
- User selectable scaling of image data (now with 2% histogram clipping linear stretch),
- Save region data to an ASCII file,
- 3 band RGB image display (2% histogram clipping linear stretch or histogram equalization),
- Overlay of cloud mask results,
- Projection onto a map base,
- Overlay of HIS field of view locations and times (requires HIS data),
- Interactive zoom and roam window,
- IDL 5.1 compatibility.

Over 50 users of the SHARP program have been confirmed outside SSEC, and several of them have expressed an interest in a similar capability for MODIS. In addition, the program was successfully used at UW in the Atmospheric and Oceanic Sciences Department for a class exercise in a graduate atmospheric radiation course that introduced students to the radiative properties of real clouds observed by the MAS.

To demonstrate the capability for global display of MODIS data, a short test program was put together using existing CIMSS IDL code. The program was run on the TLCF and accomplished the following:

- Read 42 simulated MODIS L1B granules,
- Converted Band 31 radiance to brightness temperature,
- Resampled Band 31 brightness temperature to a Global Aitoff projection.

The run time was approximately 5 minutes. This capability will be important for MODIS, as we plan to automatically generate global summary images every 24 hours. These daily images will be crucial in the quality assessment of MODIS on-orbit performance, as they will help to identify any persistent cross-scan biases, or day/night anomalies.

<u>UW MODIS SCF</u>

Silicon Graphics Origin2000 hardware for the UW MODIS SCF arrived on January 29. Components include:

- Origin2000 rack system with 2 x R10000 195MHz CPUs,
- 512 MB RAM,
- Challenge RAID with 15 x 9GB disk drives.

After an extensive testing and shakedown period, the system was made available to the UW MODIS group. This is also functioning as a compute server for other UW groups who have contributed hardware resources. The Origin has now become the primary development system for the UW MODIS group, and all MODIS algorithms have been ported successfully to Irix 6.4 and Version 7.2 compilers. In addition, the new system has allowed algorithm testing with large volumes of MAS data. Hundreds of thousands of MAS scans have now been processed successfully with prototype MODIS cloud algorithms.

The CIMSS MODIS group has adopted the Concurrent Versions System (CVS) for revision control. CVS allows simple management of source code revisions when multiple developers are working on a project.

Simulating MODIS Resolution Data

In order to assess the effects of degraded spatial resolution on MAS processing algorithms, software was developed in IDL which degrades MAS 50 meter resolution data to approximate MODIS resolution (1000 meter). To simplify processing and visualization of 1 km results, the program creates an output HDF file in exactly the same format as the input file, except that all image arrays are averaged to 1000 meter resolution and the resulting average values are replicated to give the same number of pixels and scans as the input file. This allows existing processing and visualization software to process the data.

Some surface features cause the cloud mask algorithm to fail. These sub-MODIS pixel effects can now be investigated using the averaged MAS data. As a test of these effects on a simulated MODIS data set, the cloud mask was generated for both full and reduced resolution data. Figure 1 illustrates the results. The varying spring agriculture effects, that cause the cloud mask to incorrectly flag some scenes as cloudy, almost completely disappear when the data is averaged to 1 km. Investigations of other averaged MAS tracks, where surface features have adversely affected the cloud mask, indicate that most of the problems will be alleviated with the larger MODIS footprint.

Atmosphere Group Meeting

Steve Ackerman, Rich Frey, Liam Gumley and Kathy Strabala attended the MODIS Atmosphere Group Retreat on 3-5 February in St. Michael's Maryland. Many group issues were discussed, including algorithm progress, outstanding concerns, and group science investigations. Algorithm status was presented for each UW product using results from SUCCESS and WINCE data. Critiques of the MAS cloud mask were given by the teams headed by Drs. Michael King and Yoram Kaufman. They used output from the cloud mask as input to the cloud optical properties and aerosol algorithms. The critique and ensuing discussion was very useful; it helped to identify problem areas and gave UW a better understanding of how the MODIS cloud mask will be used operationally.

MODIS Infrared Calibration

Chris Moeller and Dan LaPorte attended the MODIS IR calibration workshop held on 2-3 February in Miami. At the meeting MCST reported on progress regarding MODIS AM-1 IR calibration characterization as well as plans for FM-1 testing. Considerable progress has been made. MODIS RSR has been finalized, separate calibration for each scan mirror side is planned, and the PC band crosstalk correction algorithm has been accepted (coefficients are TBD). Experience using destriping techniques on GOES data will be used as guidance for MODIS. Modeling aft optics polarization is a continuing investigation. It was suggested that UW investigate the feasibility of using a Fourier Transform Spectrometer (FTS) for MODIS RSR measurements. It was found that optical matching of an FTS system with MODIS is feasible. It has been suggested that SBRS be authorized to proceed with a small study effort needed to resolve the data timing and schedule issues, and to develop a cost estimate for data collection, test time, and optical matching equipment. The FTS method of measuring RSR is a promising and innovative use of FTS technology and should be considered for characterizing RSR of future instruments. After the workshop, UW forwarded information on GOES destriping techniques and a revised set of BCS temperature settings for use during FM-1 T/V performance testing.

Regression coefficients relating radiance of MODIS band 28 (7.34μm) and the SWIR leak region at about 5.3μm were delivered to MCST. The relationship (Figure 2) predicts the radiance at 5.3μm as a function of MODIS band 28 radiance and this in turn is used to correct radiance leakage into MODIS SWIR bands 5, 6, 7, and 26. The relationship is based on one year of global radiosondes used in a forward model based on MODIS RSR and the MODIS Airborne Simulator (MAS) spectral band at about 5.25μm. While the relationship is a very good predictor for the majority of atmospheric conditions encountered by MODIS, it will be challenged when MODIS is viewing very dry atmospheric conditions over varying surface emissivity conditions. This relationship will be implemented for use at launch and will be supplemented by on orbit SWIR band measurements in nighttime conditions.

At the MODIS Characterization Workshop and MODIS Science Team meeting, an electronic crosstalk affecting the SWIR, MWIR and PV LWIR bands was discussed. The phenomena was outlined by MCST and preliminary estimates of the radiometric impact were provided. The crosstalk affects several bands utilized in the MODIS Cloud Mask (MOD35). These include bands 5, 6, 7, 20, 22, 26, 27 and 29. These bands are used in tests for low cloud over snow, high cloud, cloud shadows, and clouds during polar night. Also snow and aerosol screening in the cloud mask is affected.

MAS Calibration

UW and Ames Research Center (ARC) atmospherically corrected monochromator measurements of the MAS IR spectral response functions (SRF) from February 1997 have been compared to forward model calculations. Both UW and ARC use the same approach to atmospherically and spectrally correct the raw SRF measurements; however, truncation and smoothing differences are causing some variation between the UW and ARC corrected (i.e., "final") SRF. The comparison (Table 1) shows that differences in most MAS bands are less than 1% ($\Delta L/L$), with exception of bands 35 (MWIR CO_2 band), 40 and 41 (H_2O sensitive bands). Radiometric differences in bands 32, 35, 47 and 50 are primarily due to retention of SRF in the "wings" of the band while differences in bands 39-41 are primarily caused by difference in the shape of the final SRF. A detailed review of the UW and ARC SRF correction procedures will be made to remove any artifacts in the correction procedure for the final SRF.

ARC has implemented a standard procedure for spectrally calibrating the MAS instrument. This includes a spectral alignment of the four ports (VIS/NIR, SWIR, MWIR, LWIR) of MAS before every field deployment as well as the standard spectral measurement before and after each deployment. The benefit of this approach is that it "standardizes" MAS spectral characteristics going into every field deployment, and thus allows a rapid turnaround of "preliminary" calibrated data after the deployment (within weeks instead of months). The increasing use of FTS technology in the ARC calibration facility has dramatically reduced the data collection time for spectral alignment and calibration to about 1/3 of that required by the monochromator measuring system.

Fourier Transform Spectrometer (FTS) measurements of MAS SRF at the ARC calibration facility are being evaluated as a possible replacement for the traditional monochromator-based approach. Currently, both FTS and monochromator based spectral measurements are being made. The FTS system has the advantages of comprehensive spectral coverage (400 - 4000 cm^{-1}) for each measurement, improved signal to noise and spectral resolution compared to the monochromator system, and reduced time to collect the data. The comprehensive spectral coverage facilitates identification of out-of-band response in each spectral band while improved signal to noise and spectral resolution enhance definition of spectral absorption features. MAS spectral measurements using FTS were compared to monochromator measurements using data collected in February 1997. The comparison is made by simulating MAS radiances (using forward model) for the FTS and monochromator SRF. HIS data is used to define the earth-atmosphere radiance spectrum for the forward model. The simulated MAS radiances are then compared with collocated MAS inflight radiances to determine absolute calibration biases between MAS and HIS for each set of SRF. Because of enhanced spectral feature definition using the FTS system (leading to a better atmospheric correction), it was expected that FTS would improve the accuracy of MAS SRF for atmospheric bands; however, findings show that using FTS for MAS SRF measurements did not reduce absolute calibration biases between MAS and HIS for the atmospheric bands (e.g. bands 33, 34, 43, 49, 50 in Table 2). The implications of this unexpected result include possible unanticipated spectral shift of the MAS grating position sometime between the dates of February 8 and the monochromator and FTS measurements (taken a few days apart in late February), erroneous SRF

measurement by the FTS system, or inaccurate atmospheric and spectral correction of the FTS measurements. Subsequent MAS spectral characterization by FTS has been made and will be evaluated in a similar manner.

In February, a paper titled "Spectral characterization of MODIS Airborne Simulator (MAS) using an interferometer as a source" was presented to a Bomem FTS workshop held in Quebec City in February. The paper recounted the experience of ARC in applying FTS technology to making spectral measurements of the MAS instrument. While FTS usage for spectral calibration measurements is still in a maturing process, the paper outlined the benefits of applying FTS, which include simultaneous measurement of in-band and out-of-band response, improved signal-to-noise and improved spectral resolution, all with significant reduction in laboratory measurement time required.

Field Activities

The NPOESS Airborne Sounder Testbed - Interferometer (NAST-I) flew it's maiden integration missions onboard the ER-2 from Dryden Flight Research Center (DFRC) in March. NAST-I will provide scanning IR interferometer data to the Wallops98 and CAMEX-3 field programs, and is an important component of MODIS calibration validation activities. The integration missions were successfully conducted; data from these missions will be used to improve the radiometric performance of NAST-I.

Preparation and onset of the Wallops98 field deployment (26 June - 16 July) is in place. MAS will join the field experiment in the 2nd half of the deployment (July 7) and will fly with the NAST-I, HIS, and AVIRIS instruments. Primary objectives include NOAA-15 underflight for calibration validation exercise, NAST-I calibration characterization, and atmospheric moisture mapping. Two short flights are planned to accomplish these objectives. These exercises will support MODIS validation objectives after launch of AM-1. The data collection during Wallops98 is rounded out by an uplooking AERI instrument at Wallops Flight Facility, classonde launches at the AERI site, and planned ozonesonde launches at a nearby Wallops facility.

Despite a delay in the launch of EOS AM-1, MAS will be deployed on the ER-2 during the final two weeks (tentatively Sept 10-24) of CAMEX-3 (to be held in Aug/Sep 1998 from Patrick AFB, FL). One science interest is underflying NOAA-15 (launched in May 1998) carrying the new AMSU-A and AMSU-B instruments as well as infrared sounding capability. The performance of these instruments will be validated by ER-2 underflights in conjunction with surface based observations (uplooking lidar, uplooking and downlooking interferometers). CAMEX-3 also presents opportunities to monitor clouds (microphysics, heights, detection) in tropical systems with co-incident in situ data collection. The ER-2 will be equipped with a dropsonde capability for characterizing the atmosphere below the aircraft. MAS will contribute quicklook imagery and nadir brightness temperatures for selected bands as well as derived cloud products for selected case studies of interest to the CAMEX-3 community. A recent failure of the MAS Port 4 (LWIR) dewar is being assessed for possible impact on CAMEX-3 activities.

AVHRR Cloud Mask Web Site

An additional feature has been added to the display of the UW AVHRR near-real time cloud mask results at http://cimss.ssec.wisc.edu/poes/cldmsk.html. Images of NDVI (Normalized Difference Vegetation Index) are shown for clear-sky regions in portions of North and South America. In addition, weekly averages are shown for most of North and Central America that track the changes in green vegetation as the seasons progress from late winter through spring into summer. Also changes in parts of Central America during the transition from the dry to the wet season are evident. The intent is to show a practical benefit of the cloud mask and not to indicate quantitative vegetation index results.

Infrared Surface Emissivity Studies

Visiting scientist Dr. Youri Plokhenko continues his investigation of MAS temperature/moisture retrieval sensitivity to surface emissivity. He is using a physical retrieval algorithm to evaluate the effects of non-gray body surface emissivities on atmospheric temperature and humidity profiles. Good correlations between retrieved surface temperature derived using a non-uniform emissivity (reflection included) and the Normalized Difference Vegetation Index (NDVI) are found (Figure 3). The statistically significant negative correlation (-0.78) can be physically explained by an increase in vegetation density corresponding to a decrease in temperature through evapotranspiration. The scatter diagram in Figure 3 demonstrates that the surface temperature estimate obtained by the model, which includes reflection, is physically grounded. In addition, the atmospheric profile variations in space are smoother and more physical.

Cirrus Cloud Properties

Dr. Sunggi Chung continues calculating the cloud forcing expected from various cirrus cloud. A sensitivity study of high-spectral resolution infrared (IR) measurements to cirrus microphysical and macrophysical properties nears completion. Using radiosondes from the Department of Energy‘s Atmospheric Radiation Measurement (ARM)-site to specify the state of the atmosphere, high-spectral resolution measurements are simulated by combining gas optical depths from a line-by-line radiative transfer model with the discrete ordinate radiative transfer model. The sensitivity of the high-spectral resolution measurements to particle size, ice water path, cloud top location, cloud thickness, and multi-layered cloud conditions is estimated in a multitude of calculations.

Comparisons of theoretical calculations of cirrus ice cloud and interferometer measurements between 700 and 1300 cm-1 have been made for three different ice cloud situations. The observed data are from the SUbsonic aircraft Contrail and Cloud Effects Special Study (SUCCESS) by the High-spectra resolution Interferometer Sounder (HIS) mounted on NASA ER-2 aircraft flying at 20 km reported earlier (Smith et al. 1998). The

optimum number of narrow bandwidths measurements to retrieve cloud properties is the next focus of this work.

IR retrieval of cloud microphysical properties using the 8-12 micron regions have been developed. We are working with Dr. Heymsfield of NCAR to validate the retrieval of cloud particle size and ice water path. Two good case studies from the SUbsonic aircraft Contrail and Cloud Effects Special Study (SUCCESS) experiment have been identified (May 2, and April 16). Both these days have coincident data available from in-situ DC-8 microphysical measurements and passive ER-2 MAS measurements. In both these cases, the DC-8 can be identified in the MAS imagery.

Cloud Thermodynamic Phase Modeling

Dr. Bryan Baum, in Madison as a visiting scientist from NASA LaRC, is assisting in the modeling of microphysical properties in a series of MODIS channels, with the goal of assessing and improving the MODIS microphysical cloud phase retrieval algorithms. He has set up a discrete ordinates radiative transfer (DISORT) code to model six of the MODIS/MAS bands at 0.65, 1.6, 3.8, 8.5, 11, and 12 microns. This model employs a set of correlated k-distribution routines to accurately depict atmospheric gaseous absorption due to water vapor, nitrous oxide, methane, and other pertinent trace gases. Water droplet cloud optical properties were generated through application of Mie theory. To simulate cirrus clouds, a set of optical properties (e.g., single scattering albedo, extinction coefficient, and phase functions), developed by researchers at the University of California at Los Angeles, were used. With the DISORT model, relationships between measurements at the chosen wavelengths can be explored. Figure 4 shows sample calculations derived for a case study of cirrus for the SUCCESS time period. Note the large brightness temperature differences that cirrus clouds exhibit in the 3.8-8.5 micron panel. This channel combination is being investigated as an improvement to the tri-spectral technique.

DATA ANALYSIS

Cloud Properties Algorithm Development and Testing

Completion of the UW MODIS production software deliveries has permitted the UW group to concentrate on science data processing and algorithm testing. Both the cloud phase and cloud top properties algorithms have been revised to use the MAS HDF cloud mask product as input. Scenes from both WINCE and SUCCESS are being used in the analyses. One scene is the MAS SUCCESS flight segment #28 (21:36:48 - 21:41:01 UTC) from 2 May 1996. Wave clouds, isolated cumulus clouds, and even contrails can be observed in the scene. This segment is of particular interest as validation data from both the ER-2 CLS and the DC-8 microphysical instruments are available. Wave clouds formed over the Colorado Rockies this day due to strong Northwest flow at 500 hPa. The

DC-8 and ER-2 aircraft were deployed on a mission to fly stacked patterns over and through the wave clouds.

Wave clouds are clearly evident as cold cloud with diffuse edges in the 11 micron image (Figure 5, left panel). A narrow contrail is apparent across the top of the image horizontally. Another contrail is faintly visible entering the large wave cloud from the top right part of the image. This is the trail of the DC-8, which is actually sampling within the cloud during the ER-2 overpass.

The MAS versions of the MODIS cloud mask, cloud top property and cloud infrared phase algorithms were applied to the selected track. Both the cloud top property and cloud phase algorithms used results from the cloud mask to decide when they would be implemented. Each performed retrievals on a 10 x 10 pixel region. If more than 20 of the pixels were flagged as uncertain or cloudy by the cloud mask, then the radiances of the 10 x 10 box were averaged (to reduce noise) and a retrieval was made. The three center panels of Figure 5 show results from the cloud mask and cloud top properties overlaid on the 11 micron brightness temperature image. Shaded regions in the cloud mask panel indicate pixels which were identified as uncertain or cloudy. The mask is of good quality when compared with the 11 micron image. All parts of the wave cloud, cumulus and contrails are flagged as cloudy. Certain land features in the middle left portion of the scene are flagged as cloudy; these are bright landmarks identified as cloud by the visible reflectance tests. These feature affects disappeared when the cloud mask was run on the same MAS data set averaged to MODIS resolution (1 km) (See Figure 1).

MAS CO_2 cloud top pressures and effective cloud amounts for the May 2 flight track are shown in the right image panels of Figure 5. Wave cloud top pressure retrievals consistently lie between 200 and 300 hPa, except near the top edge of the large wave cloud, where the tops lower to 300-400 hPa. Effective cloud amounts (or effective emissivities) range from very small around the edges of the wave clouds (10-20 %) to large (80-90 %) in the center of the clouds. Cloud amounts of 100 and cloud heights of 800 hPa dotting the edges of the clouds and in the contrail are due to the window channel solutions in areas where the cloud forcing is too small (within instrument noise). When the 10 x 10 pixels are averaged, these very thin clouds will have a very similar radiance as that of the calculated clear values. To alleviate this problem, the MODIS version of the CO_2 slicing will not allow the window channel solution to be used unless all pixels in a given 5 x 5 pixel box are flagged as cloudy. Cumulus cloud retrievals are generally as expected, with cloud heights lower and cloud amounts greater than the wave clouds.

The rightmost panel of Figure 5 is a graph of nadir cloud heights from both the ER-2 Cloud Lidar System (CLS) and MAS CO_2 slicing. The CLS algorithm detects a maximum of five cloud top and cloud bottom altitudes based upon the backscatter signal. In the graph, the highest two detected cloud tops are plotted. The different techniques compare favorably over much of the scene. There are stretches however, where the cloud mask did not detect cloud, but the CLS was detecting very thin cirrus. Both techniques retrieve cloud heights for most of the wave clouds at 12 km. The main exception is near the end

of the track, where the CO_2 heights drop. In this case, a second, and even third and fourth cloud deck is found (not shown). In multi-layer cloud layer situations, the CO_2 slicing technique will calculate a cloud top pressure in between the top and bottom layer. However, as is discussed below, the CO_2 and lidar heights compare favorably with little to no bias.

An improvement has been made to the method when retrieving pressure altitudes of low clouds. It was noticed that some unrealistically high cloud altitudes were obtained when the scene included low-level water clouds. These results were due to inappropriate utilization of the 11/13 μm channel combination for water clouds where they have differing cloud emissivities at these two wavelengths. A check on the difference between the 8 and 11 μm brightness temperatures can provide a way to make sure the scene contains only ice cloud. If the 8 - 11 μm brightness temperature difference is less than 2 degrees, indicating water clouds, the 11/13 μm cloud height solution will not be used. The same change will be made to the MODIS algorithm. The first draft of a manuscript describing these results has been written and will be submitted for publication in the 3rd quarter 1998.

CO_2-slicing cloud heights are being validated in comparisons with cloud heights derived from Cloud LIDAR System (CLS) data for all MAS flight lines where both the MAS and the CLS were operating normally. Only MAS CO_2-slicing results from near the nadir position could be compared because the CLS is not a scanning instrument. Longwave infrared MAS radiances (channels 45, 48, 49, 50) were averaged over 10X10 pixel groups for input to the MAS cloud height algorithm. Initial results of the validation are favorable. Figure 6 shows a histogram of the cloud height differences (LIDAR minus CO_2-slicing) between the two methods.

Cloud phase retrievals from the 2 May flight track were generated for MAS viewing angles less than 20 degrees. The results are shown in Figure 7. The quality of the results are mixed. The majority of the wave clouds, which are high and cold and composed of small ice crystals, are flagged as either thin or thick ice cloud (values 4 and 2 in Figure 7). As you proceed towards the edge of the wave clouds, the technique flags pixels as either mixed phase (3) or non-opaque water cloud (5). The reason for this is that a good linear fit was not possible for 8 minus 11 micron versus 11 minus 12 micron brightness temperature differences. As a result, the technique defaults to a pixel by pixel cloud phase discrimination. Ambiguities in the scatter diagram for thin cirrus and water cloud cause misidentifications. Work continues on ways to improve phase determinations in mixed-phase and multi-layer cloud situations.

Cloud Mask Evolution

Several enhancements and/or changes have been made to the MAS cloud mask software. A different visible thin cirrus test threshold has been implemented that allows more cirrus to be designated as “thin” (bit #9 in the cloud mask output file) and less to be classified as “cloudy” (bits 1-2).

A global ecosystem map at 1 km resolution (analogous to the 1 km land/sea tag file from the USGS) may now be used as input to the cloud mask. The option is specified on the command line when running the program.

The non-cloud obstruction test is now performed only in appropriate regions of South America (as in SCAR-B data) and "forest" ecosystems (according to the ecosystem map). This helps eliminate false determinations of smoke and aerosol over many North American grassland and cropland scenes (as in SUCCESS data).

The MAS cloud mask was used during the FIREACE experiment by Dr. Michael King's group when their cloud retrieval algorithm could be applied. MAS port 4 data (longwave infrared channels) were missing for several days, which caused the cloud mask to fail. As a result, more rigorous bad data checks have been added to the MAS cloud mask code. Figure 8 is an example of the MAS cloud mask from a day where port 4 data was not collected. This scene, from 20 May 1998, had some reasonable radiance values which incorrectly appeared in port 4 channels; these values are the bright bands in the 11 micron image of Figure 8. It was impossible to filter these values out, which caused the banded structure in the cloud mask result. Where port 4 data values were sufficiently unrealistic (near zero), the cloud mask performed quite well using just visible and near-infrared tests (Figure 8).

MAS data from the WINCE experiment is being processed more thoroughly and the cloud mask results are being examined carefully. This unique daytime winter and nighttime winter data set will be used in the development of the polar and nighttime MODIS algorithms. An example of the cloud mask applied to a difficult winter scene is shown in Figure 9. The winter of 1996-1997 was a brutal one over the Dakotas, with record heavy snow and cold. The ER-2 overflew this area on 12 February 1997. The cloud mask for this scene illustrates the ability to detect very thin cirrus over a very cold background.

Confidence in the good quality of the MAS cloud mask is now high after tests with almost every 50 channel MAS data set. A new version of the mask that includes the above additions, will be released 3rd quarter 1998.

MODIS Infrared Calibration

At the February MODIS IR calibration workshop, PFM PC band crosstalk was discussed with a goal of identifying an acceptable correction algorithm for use in the MODIS L1B data production software. The analysis of correction coefficients for use in the correction algorithm was also discussed. Data analysis indicates that a linear correction approach is acceptable. The proposed correction algorithm makes the correction at the digital number (DN) level of the calibration process. Importantly, DN must be corrected for all scenes (EV, SVP, BB). The proposed algorithm is

$$DN^{true}(i,j) = DN^{cont}(i,j) - Xtalk * DN(31,j) * p(i,j) + q(i,j) \quad (1)$$

where DN^{true} and DN^{cont} are the non-crosstalk affected DN and the crosstalk contaminated DN respectively for band i channel j, Xtalk is the crosstalk amplitude from band 31 channel j to band i channel j, DN(31,j) is the DN for band 31 channel j, and p and q are placeholders for post-launch adjustments to the algorithm (set to 1.0 and 0 resp. at launch). The spatial dependence of the crosstalk from the band 31 leak source and the receiving band i is not expressly shown in eqn (1) but is included in the correction algorithm.

An approach using the PFM RC-02 radiometric performance test data sets has not been successful in uniquely retrieving the value of Xtalk (i.e. the crosstalk coefficient) for each PC band, but has contributed to formulating the correction algorithm and gaining insight into PC band crosstalk effects on performance test data. The pre-launch PC band radiometric calibration coefficients will be adjusted to remove influence of PC band crosstalk. A new approach for identifying the value of Xtalk for each band has been proposed by MCST. This physical approach is based on the expectation that same-family detectors should exhibit very similar nonlinearities. Preliminary findings are in line with anticipated crosstalk amplitudes of the various PC bands based on analysis and experience with other PFM test data sets. The assumption of similar nonlinearities in same family detectors will be tested by analyzing data from FM-1 performance tests; PC band crosstalk in FM-1 is expected to be small compared to that of PFM.

On orbit determination of PC band crosstalk amplitude is currently focused on the use of moon view data. MODIS will view the moon in its various phases on a regular basis (approximately monthly) through the SVP. That data will be used in a regression analysis of the Xtalk coefficient through applying a rearranged eqn (1) to scenes in which DN^{true} is constant (i.e., when DN^{true} is the deep space background). It is anticipated that band 31 will be illuminated by the moon when other PC bands are viewing cold space. Two data points (one band 31 on the moon and one band 31 viewing deep space) can be used to solve the linear system for the Xtalk coefficient as the slope of DN(31,j) versus DN(i,j). A timeseries of Xtalk estimates will be produced and reviewed for stability. These Xtalk estimates can be applied, initially on a trial basis, in the L1B radiance algorithm and evaluated. An improved crosstalk correction will be sought. Another methodology, applying large samples of earth view data can be used as a sanity check. Using forward model radiances (from radiosonde or model data), a global data set of radiances for MODIS band 35 (inband only) can be generated and analyzed with MODIS band 35 observations to estimate the crosstalk coefficient. Synergism with the GOES satellite CO_2 bands will also be explored.

Evidence of electronic crosstalk has been observed in PFM and FM-1 IAC performance test data sets at UW. Leakages in the PV LWIR bands (27-30) were observed. As opposed to the PC LWIR band crosstalk, the PV LWIR band leaks were observed at the inband spatial position (i.e detector illuminated) of other PV LWIR band detectors; for PC LWIR band crosstalk, the leak was observed at an edge near the band 31 detector. The

PV LWIR band crosstalk observed at UW is consistent with the findings presented by MCST at the MODIS Characterization Workshop and Science Team meeting in June.

GOES Biomass Burning Program

The following work is being funded under separate NASA (NAG5-4751) and NOAA contracts. It has relevance to the MODIS biomass burning investigations.

Diurnal multispectral GOES-8 imagery collected over South America during the 1997 fire season (June-October) were processed with the GOES-8 Automated Biomass Burning Algorithm (ABBA, version 5.6). The 1997 GOES-8 ABBA results were compared with results for 1995 as part of an ongoing study to document spatial, diurnal, and interannual trends in biomass burning in South America (Prins et al., 1998 a, b). Composites of GOES-8 ABBA processed, saturated, cloudy, and high-probability possible fire pixels and estimated burned area detected at 1745 UTC during the 1995 and 1997 fire seasons show similar burning patterns (See Figure 10). Results displayed on a .25° grid show much of the burning occurred along the perimeter of the Amazon in the Brazilian states of Maranhao, Tocantins, Para, Mato Grosso, Amazonas, Rondonia, and Acre and in Bolivia, Paraguay, and Northern Argentina. The composites (panels a-d) show distinct burning patterns along rivers and in areas with recent road construction (locations A and B). Difference plots (panels e and f) show that more fires were detected in Rondonia, Brazil and Paraguay (locations B and C) in 1995 than 1997. Increased burning was observed in Amazonas, Brazil (locations A and D) and in eastern Brazil (location G) in 1997. The distribution of burning by ecosystem type was nearly identical in 1995 and 1997. Over 90% of the burning occurred in 6 ecosystem types. The majority of the fires were located in seasonal tropical broadleaf forests (34%-1995, 33%-1997); savanna/ grassland/seasonal woods (27%-1995, 25%-1997); mild/warm/hot grass/shrub (19%-1995, 22%-1997); and succulent and thorn woods or scrub (7%-1995,1997). Overall, the GOES-8 ABBA results indicated an 8% decrease in GOES-8 ABBA observed fires from 1995 to 1997. GOES-8 ABBA results for 1995 and 1997 are available on-line at http://cimss.ssec.wisc.edu/goes/burn/abba.html. This web site also contains fire products for the 1998 fire season in near real time.

GOES-8 data were used to catalogue the extent of smoke coverage in South America during the 1995 and 1997 fire seasons (Prins et al., 1998a, b). Multi-spectral GOES-8 data collected daily during the 1995 and 1997 fire seasons (June - October) were processed with the GOES-8 Automated Smoke Aerosol and Detection Algorithm (ASADA). ASADA estimates for both years showed a gradual increase in smoke/aerosol coverage during the last half of July with maximum values (covering over 7 million km^2) in August and September corresponding to the peak in the burning season. In both years the regions most often impacted by smoke were collocated with or downwind of the most intensive burning areas. Seasonal composites of the GOES-8 ASADA product for 1995 and 1997 are shown in Figure 11. Results displayed on a .5° grid show the highest smoke/aerosol occurrences (panels a and b) and albedo estimates (panels c and d) along the front range of the Andes Mountains and along the boundary between forest and

grassland in north-central Brazil. Transport over the ocean was more pronounced in 1995. In both years the highest derived albedo estimates are 2 to 3 times higher than background values with slightly higher values in 1995. The composites closely reflect similarities and differences in burning as observed in the GOES-8 ABBA results for 1995 and 1997. Activities are underway at CIMSS to create an improved algorithm for smoke and cloud identification and a GOES aerosol optical thickness (AOT) algorithm (NASA grant NAG5-4751). These algorithms will enable better discrimination between smoke and clouds, identification of cloud type and fraction, and quantitative characterization of aerosols associated with biomass burning using GOES.

PAPERS

Ackerman, S. A., K. I. Strabala, W. P. Menzel, R. A. Frey, C. C. Moeller and L. E. Gumley, 1997: Discriminating Clear-sky from Clouds with MODIS. Submitted to the Journal of Geophysical Research.

Ackerman, S. A., S. Pryzbylak, K. T. Kriebel and H. Mannstein, 1997: A comparison of cloud water content derived from satellite retrieval techniques and surface observations. Submitted to Remote Sensing Environment.

Ackerman, S. A., C. C. Moeller, K. I. Strabala, H. E. Gerber, L. E. Gumley, W. P. Menzel, S-C. Tsay, 1997: Retrieval of effective microphysical properties of clouds: a wave cloud case study. Accepted for publication in Journal of Geophysical Research Letters.

Chung, S., S. A. Ackerman, P. F. van Delst and W. P. Menzel: 1998: Cloud characteristics inferred from model calculations compared to HIS measurements. Submitted to the Journal of Applied Meteorology.

King, M. D., S.-C. Tsay, S. A. Ackerman and N. F. Larsen, 1997: Discriminating Heavy Aerosol, Clouds, and Fires During SCAR-B: Application of Airborne Multispectral MAS Data. Submitted to the Journal of Geophysical Research.

Plokhenko, Y. and W. P. Menzel, 1998: The effects of surface reflection on estimating the vertical temperature – humidity distribution from spectral IR measurements. Submitted to the Journal of Applied Meteorology.

Prins, E.M., W.P. Menzel, and J.M. Feltz, 1998a: Characterizing Spatial and Temporal Distributions of Biomass Burning Using Multi-spectral Geostationary Satellite Data, Ninth Conference on Satellite Meteorology and Oceanography, Paris, France, 25-29 May, 1998, pp. 94-97.

Prins, E.M., J.M. Feltz, W.P. Menzel, and D. Ward, 1998b: An overview of GOES diurnal fire and smoke results for SCAR-B and the 1995 fire season in South America. Accepted by the Jour. of Geo. Res. Atmos., SCAR-B special issue.

Riggs, G. A., D. K. Hall , S. A. Ackerman, 1997: Sea Ice Detection with the Moderate Resolution Imaging Spectroradiometer Airborne Simulator (MAS). Submitted to Remote Sensing Environment.

Smith, W. L., S. A. Ackerman, H. Revercomb, H. Huang, D. H. DeSlover, W. Feltz, L. Gumley and A. Collard, 1997: Infrared spectral absorption of nearly invisible cirrus clouds. Accepted for publication in Journal of Geophysical Research Letters.

MEETINGS

Chris Moeller and Dan LaPorte attended the MODIS IR Calibration Workshop held on 2-3 February in Miami, FL.

Steve Ackerman, Liam Gumley, Rich Frey and Kathy Strabala participated in the MODIS Atmosphere Group Retreat held on 3-5 February in St. Michael's Maryland.

Dan LaPorte attended a MODIS FM-1 Environmental Review meeting at Santa Barbara Remote Sensing (SBRS), 11-12 May.

Chris Moeller, Dan LaPorte and Liam Gumley attended the MODIS Characterization Workshop on 23 June held at GSFC.

Liam Gumley attended the MODIS visualization meeting on 23 June held in Greenbelt, Maryland.

Steve Ackerman, Chris Moeller, Dan LaPorte, Liam Gumley and Kathy Strabala attended the MODIS Science Team meeting on 24-26 June in Greenbelt, Maryland.

Table 1. Comparison of UW and ARC processed SRF for IR bands.

band No.	Wavelength (μm)	L_{ARC} (W/m2 sr μm)	L_{UW} (W/m2 sr μm)	ΔL (W/m2 sr μm)	ΔL / L (%)	ΔT (K)
27	3.26	0.0636	0.0636	8E-05	0.13	0.08
28	3.41	0.1584	0.1596	-0.0012	0.78	-0.08
29	3.57	0.2861	0.2868	-0.0008	0.27	0.03
30	3.73	0.4160	0.4177	-0.0016	0.39	-0.03
31	3.88	0.5616	0.5639	-0.0024	0.42	-0.04
32	4.05	0.6922	0.6988	-0.0066	0.95	-0.23
33	4.20	0.3279	0.3279	-1E-05	0.00	-0.01
34	4.36	0.0824	0.0824	-1E-05	0.01	0.02
35	4.52	0.5366	0.5563	-0.0197	3.68	-0.75
36	4.67	1.3781	1.3840	-0.0059	0.43	-0.02
37	4.83	1.4341	1.4384	-0.0043	0.30	-0.02
38	4.98	1.6230	1.6288	-0.0058	0.36	-0.09
39	5.14	1.4331	1.4433	-0.0102	0.71	-0.17
40	5.28	1.2570	1.2736	-0.0166	1.32	-0.28
41	5.40	1.1526	1.1782	-0.0256	2.22	-0.59
42	8.52	8.7376	8.7491	-0.0115	0.13	0.03
43	9.71	6.2289	6.2282	0.0007	0.01	0.02
44	10.50	9.5350	9.5386	-0.0036	0.04	-0.05
45	11.00	9.3618	9.3534	0.0084	0.09	-0.02
46	11.99	8.6394	8.6190	0.0204	0.24	0.03
47	12.88	7.5146	7.5358	-0.0212	0.28	-0.23
48	13.28	6.1700	6.1730	-0.0030	0.05	-0.04
49	13.81	4.0881	4.0837	0.0044	0.11	0.07
50	14.26	2.6642	2.6547	0.0095	0.36	0.19

Table 2. MAS-HIS biases based on monochromator and FTS SRF. Only bands for which commensurate HIS radiance data is available are shown. Simulated MAS radiances (convoluted MAS SRF with HIS radiance spectra) were compared to collocated MAS observations using clear sky data scenes over Lake Huron on 8 Feb 1997. The monochromator based and FTS based biases are small and comparable for window bands (e.g. bands 31, 44, 45); spectral sensitivity in window bands is small. The more spectrally sensitive atmospheric band biases are larger for FTS than monochromator based SRF (e.g. bands 33, 34, 43, 50). This suggests that the quality of the Feb 1997 FTS based SRF may be lower than the monochromator based SRF.

MAS Band	Wavelength (μm)	MAS scene temp (K)	HIS scene temp (K)	MAS-HIS bias monochromator (K)	MAS-HIS bias FTS (K)
30	3.73	273.61	269.76	3.85	4.41
31	3.88	272.36	273.29	-0.93	-0.92
32	4.05	269.85	270.98	-1.12	-1.73
33	4.20	248.70	249.27	-0.58	-2.97
34	4.36	227.09	225.80	1.29	3.76
35	4.52	253.38	254.74	-1.36	1.48
36	4.67	269.20	270.09	-0.90	-1.35
37	4.83	267.82	268.61	-0.79	-0.46
42	8.52	272.23	272.65	-0.42	-0.44
43	9.71	258.30	257.96	0.33	1.69
44	10.50	273.81	274.01	-0.20	-0.19
45	11.00	273.86	273.99	-0.13	-0.15
46	11.99	273.49	273.52	-0.03	-0.04
47	12.88	271.20	271.24	-0.04	-0.19
48	13.28	262.13	262.22	-0.09	0.12
49	13.81	243.67	242.29	1.38	1.45
50	14.26	225.44	223.74	1.70	2.95

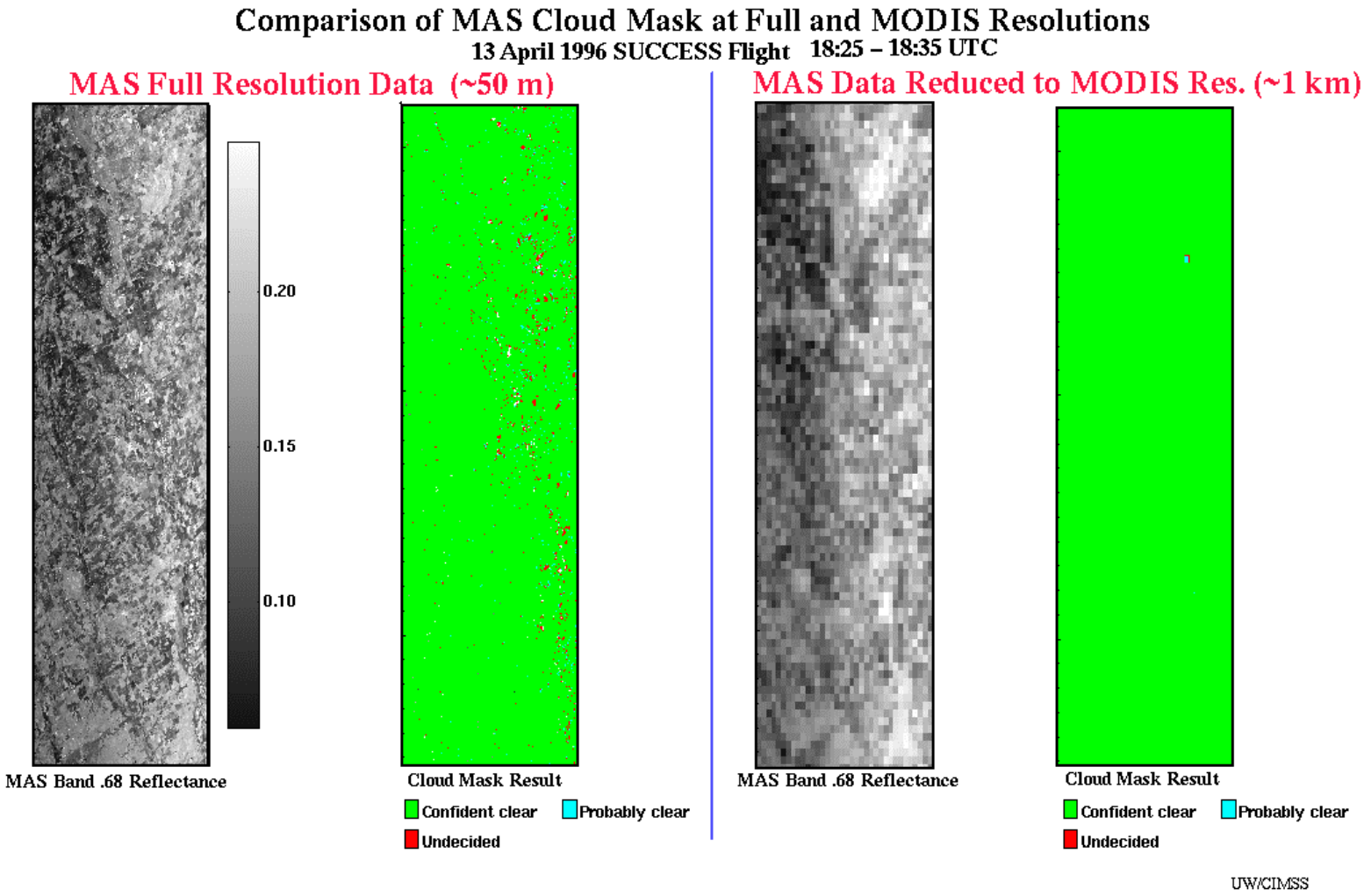

Figure 1. Comparison of cloud mask results between the full resolution MAS data (left panels) to that of the reduced MODIS-like MAS averaged data (right panels). Note how some clear scenes are incorrectly flagged in the 50 m data; these problem areas all but disappear when applied to the MODIS resolution data set.

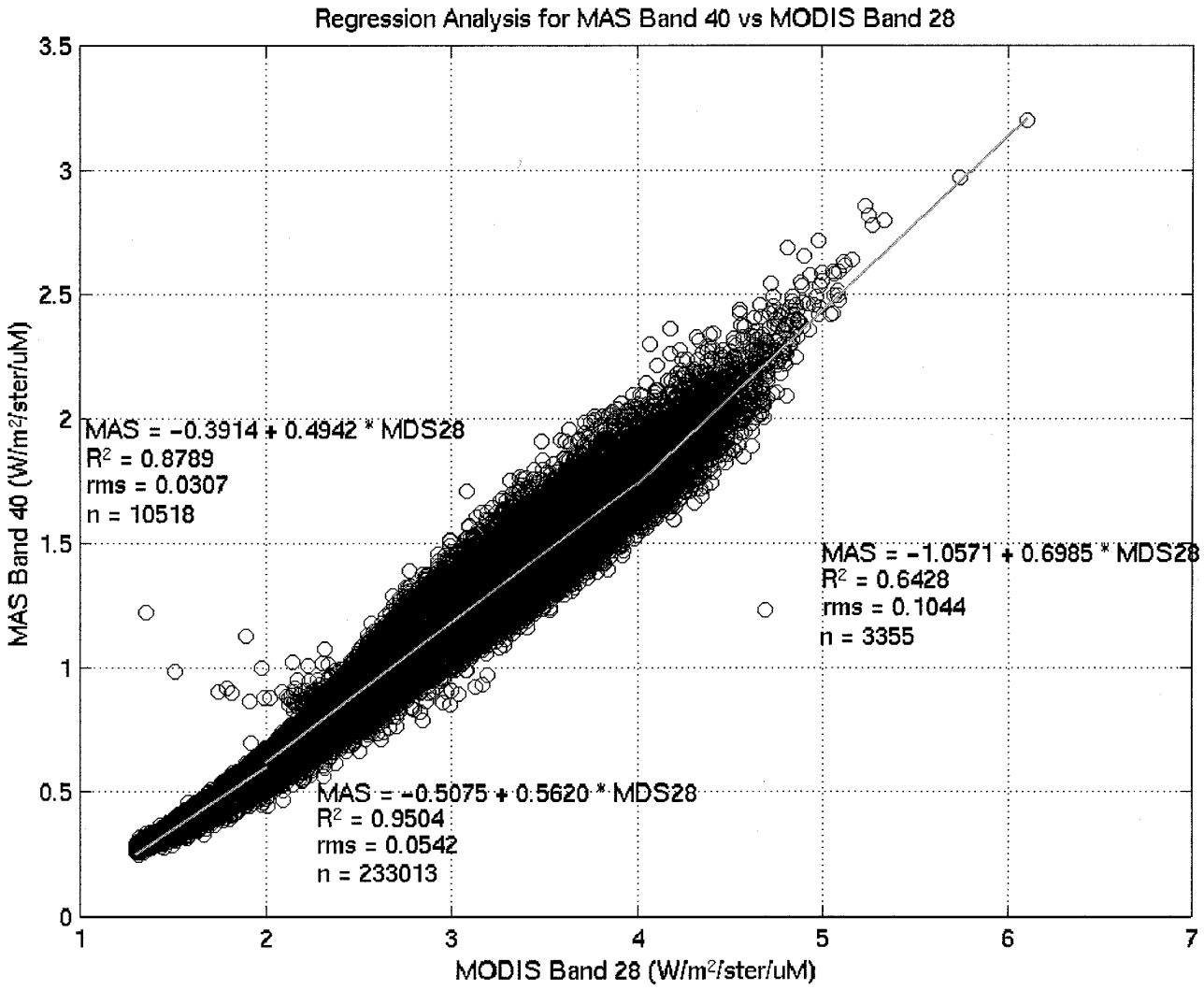

Figure 2. Relationship between MODIS band 28 and 5.3µm radiance as represented by MAS band 40. The data used in the chart are simulated radiances for one year of global radiosonde data. Very cold to very warm conditions are represented in the global sample. Separate regressions will be used for cold, moderate, and warm scene temperatures.

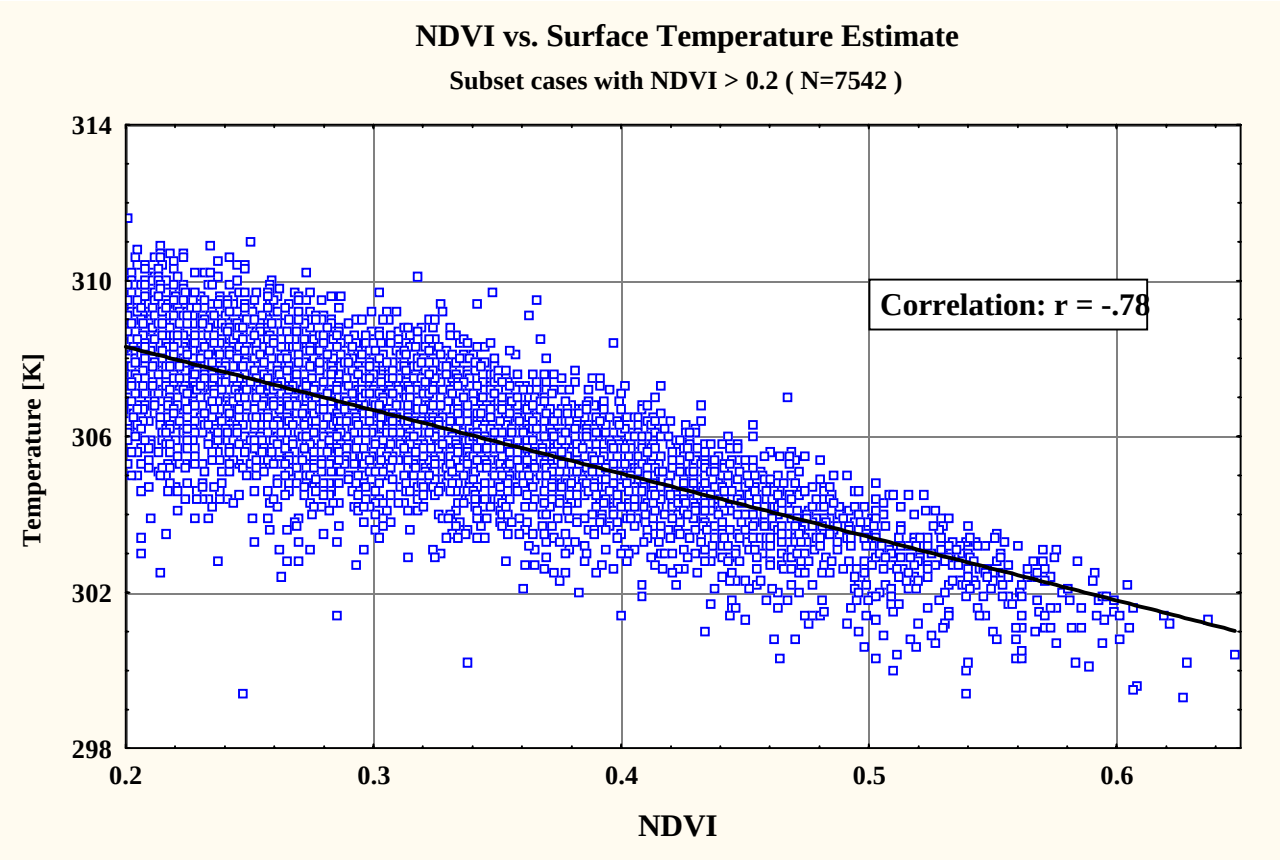

Figure 3. Scatter diagram of retrieved surface temperature, which includes surface reflection, versus the Normalized Difference Vegetation Index (NDVI) derived from a MAS SUCCESS flight from 13 April 1996.

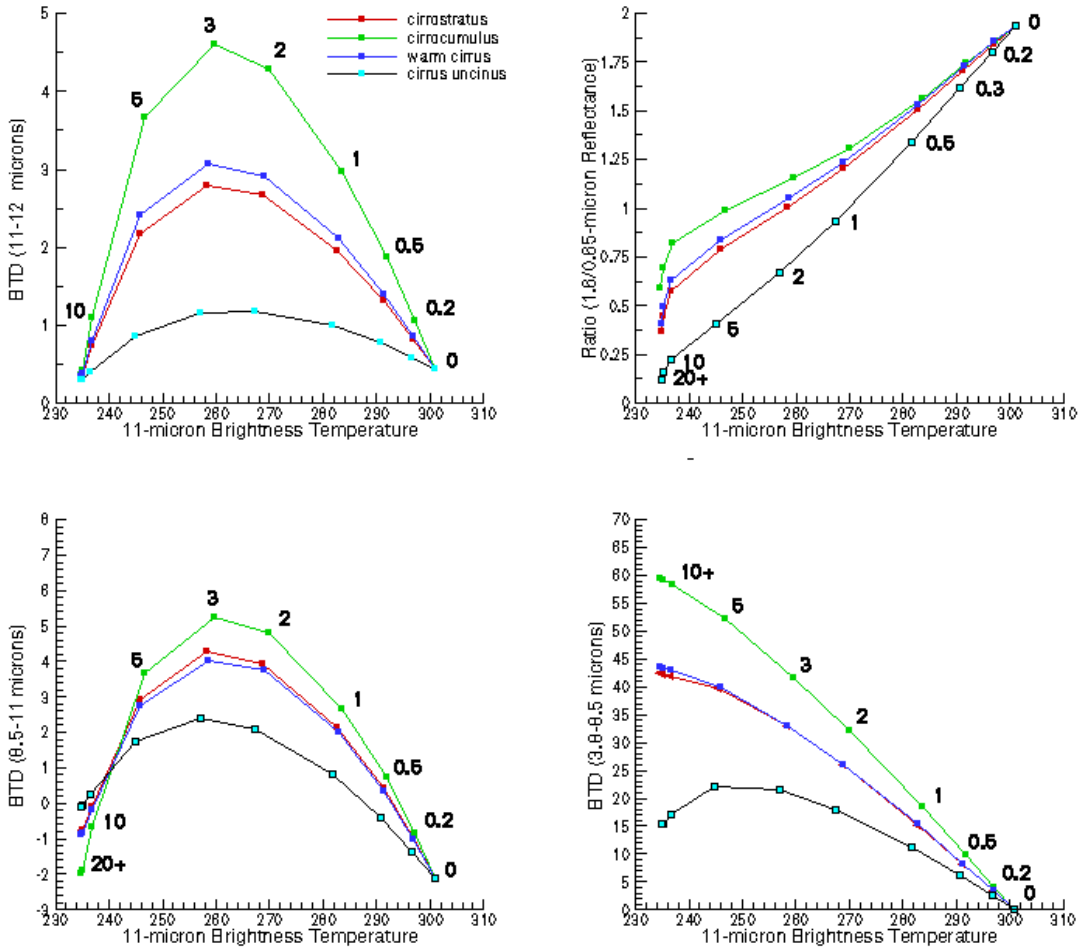

Figure 4. Discrete Ordinates Radiative Transfer (DISORT) model results of differing cirrus types and differing optical depths for MODIS/MAS channel combinations which will be used for cloud phase retrievals. The bottom right panel combination of $BT_{3.8} - BT_{8.5}$ is being investigated for its potential to improve the tri-spectral technique. Note the huge brightness temperature difference signal in this channel combination for all different cirrus types.

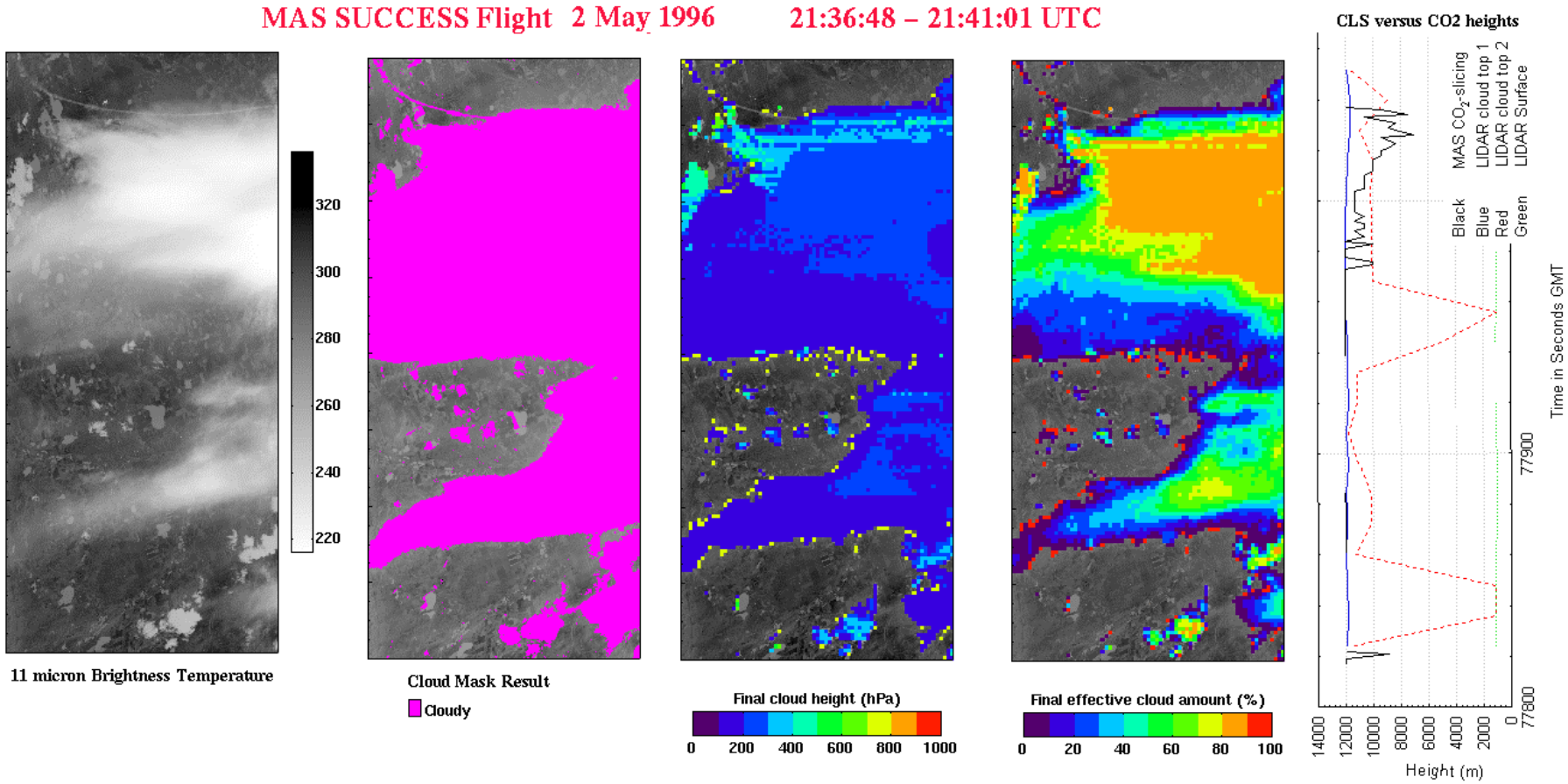

Figure 5. Example of the UW MODIS algorithm testing using MAS data, including validation. The leftmost panel is an 11 micron image including temperature scale. The middle three image panels are product results (cloud mask, cloud top pressure and cloud effective cloud amount) retrieved from the scene. The rightmost panel shows a comparison of cloud height retrievals between the MAS and Cloud Lidar System (CLS) onboard the ER-2.

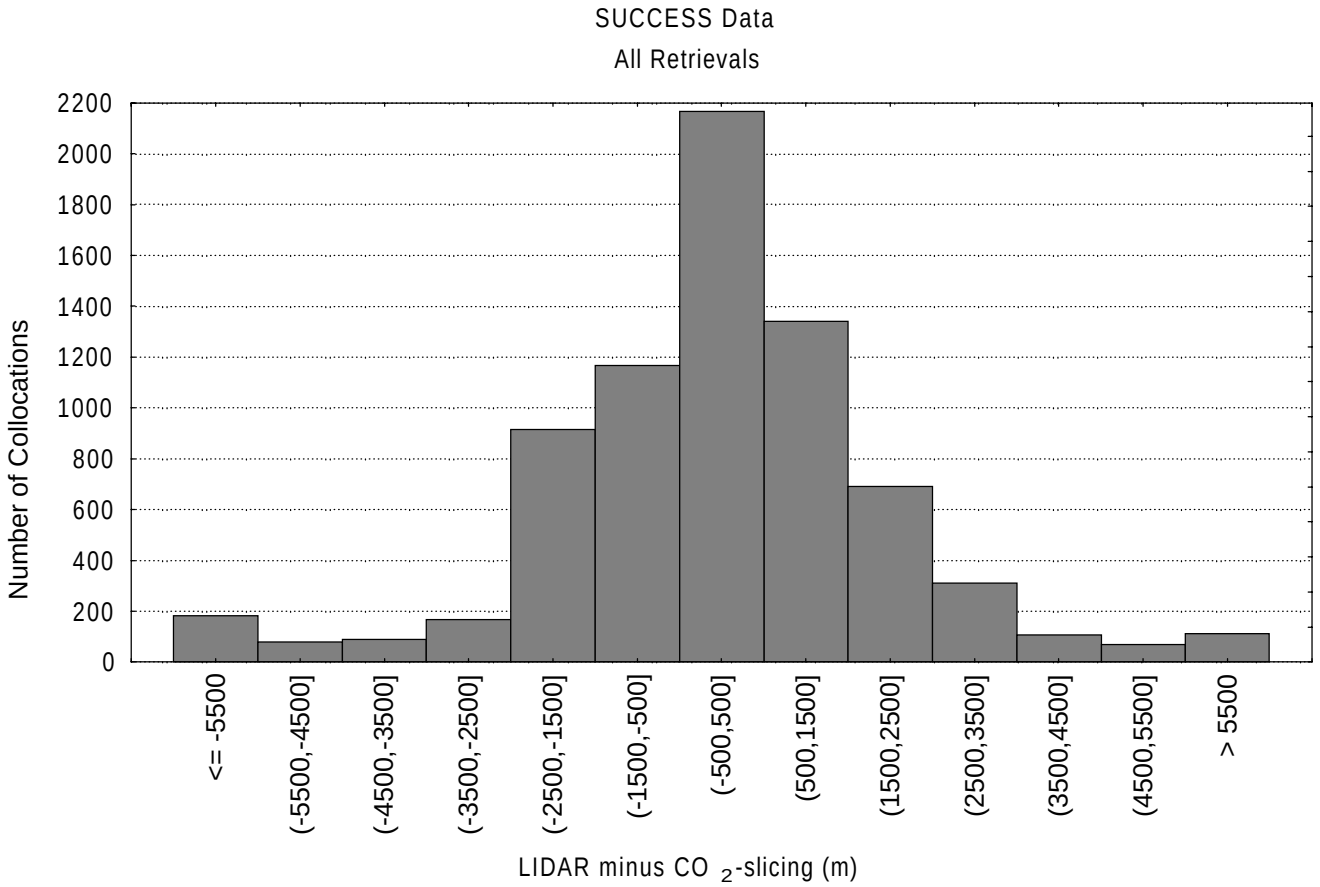

Figure 6. Comparison of MAS CO2 slicing cloud heights and heights derived from Cloud Lidar System (CLS) data. Note the Gaussian shape of the results, indicating good agreement with no bias between the results.

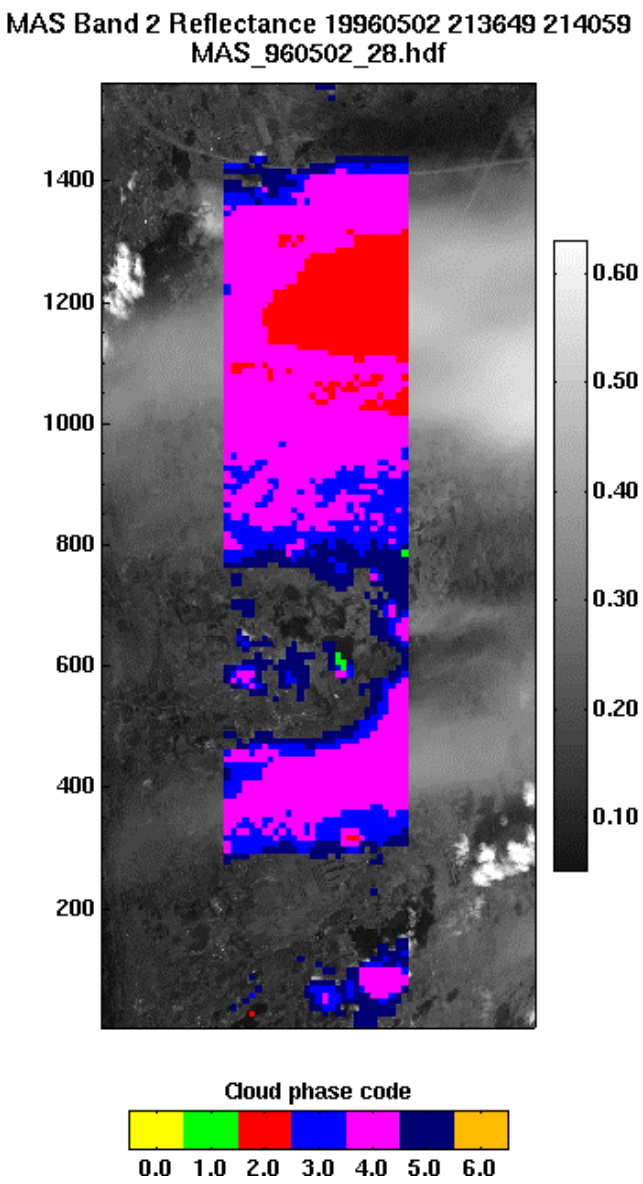

Figure 7. Results of the MAS cloud phase algorithm when applied to the same scene as shown in Figure 5. The cloud phase code stands for: 1) opaque water cloud 2) opaque ice cloud 3) mixed phase cloud 4) thin ice cloud 5) thin water cloud 6) uncertain.

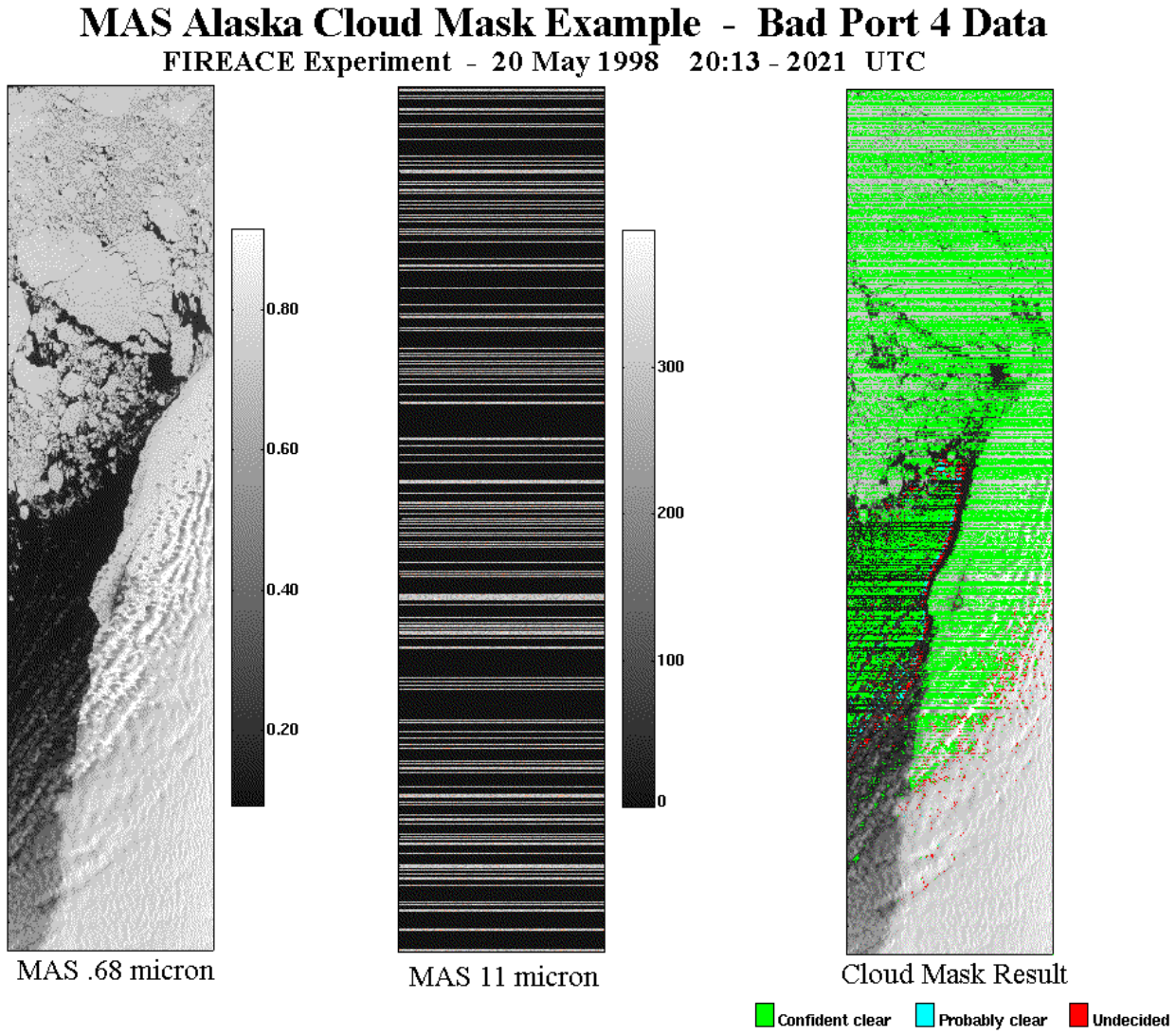

Figure 8. MAS FIREACE cloud mask example where port 4 data (longwave infrared) was not collected. Areas in the cloud mask image where the surface can be seen indicates cloud was found. The cloud mask banded structure is due to "reasonable" values incorrectly appearing in port 4 data.

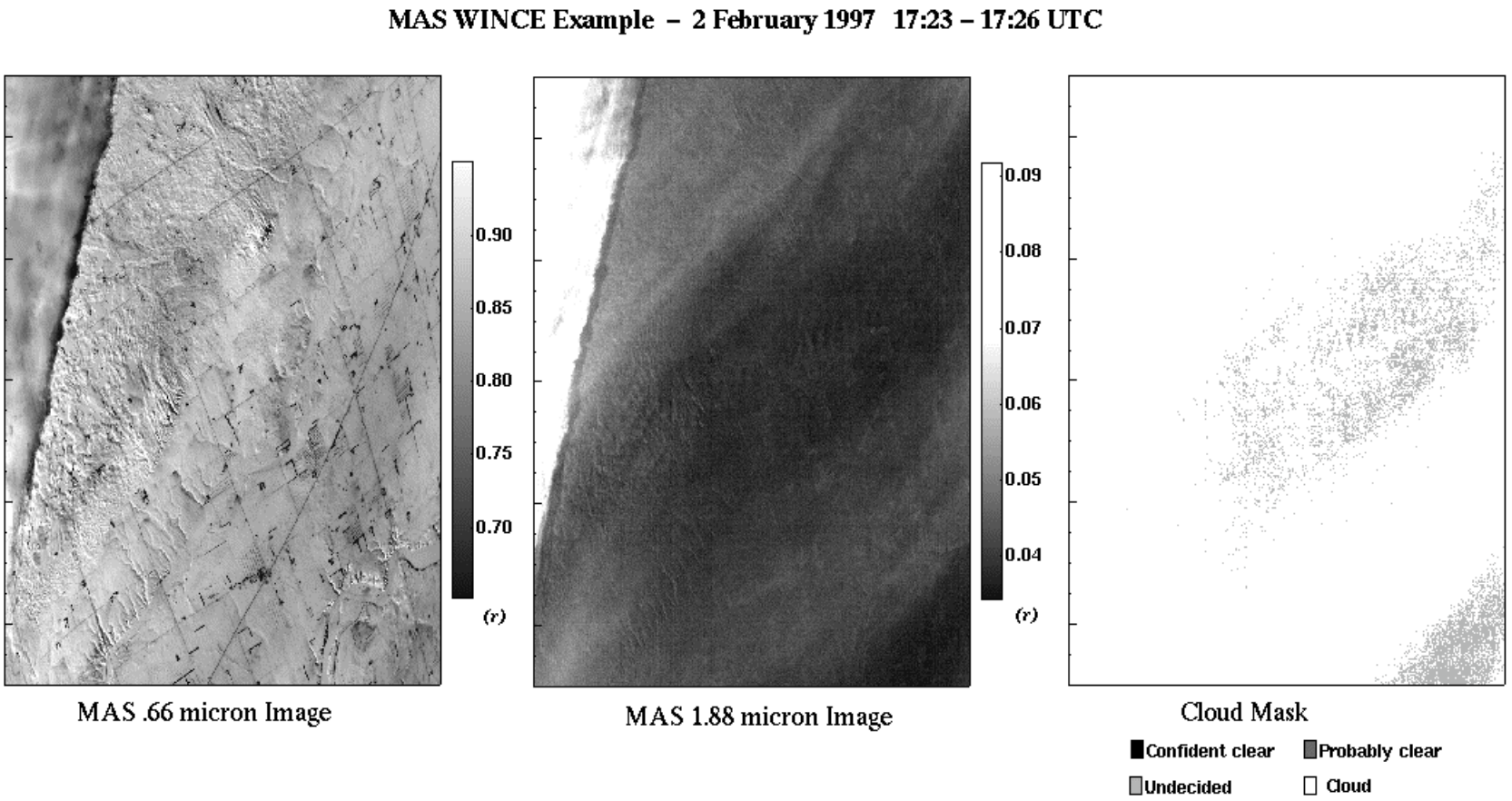

Figure 9. Example of the cloud mask applied to a very cold snow covered scene. Thin cirrus covers the entire scene, as shown in the 1.88 micron image. The cirrus is detected by the MAS cloud mask algorithm, as shown in the right most panel.

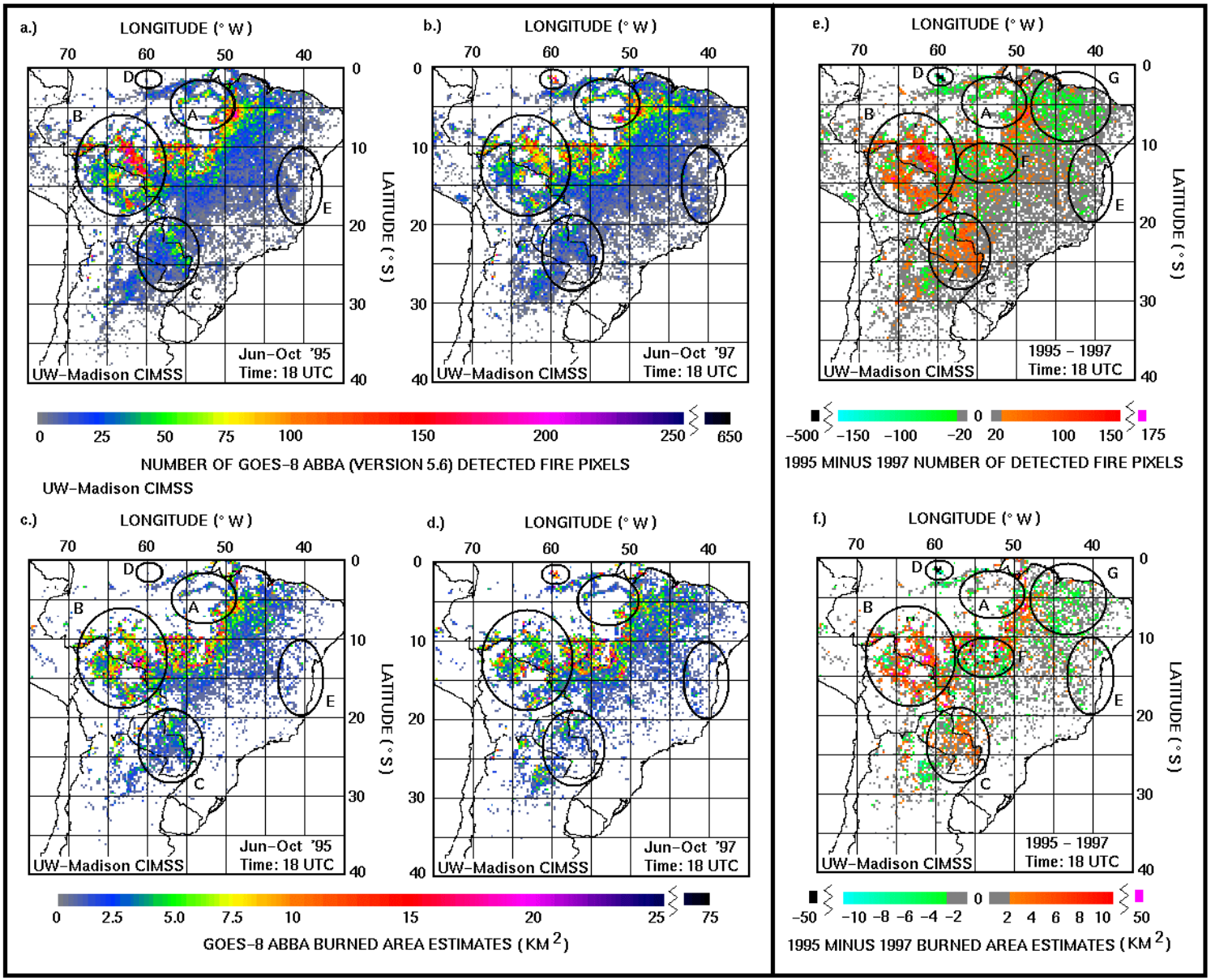

Figure 10. Composites a-d show the distribution of GOES-8 ABBA fire pixel counts and burned area estimates at 17:45 UTC for the 1995 (a,c) and 1997 (b,d) fires seasons on a .25 degree grid. Difference plots are shown in composites e and f.

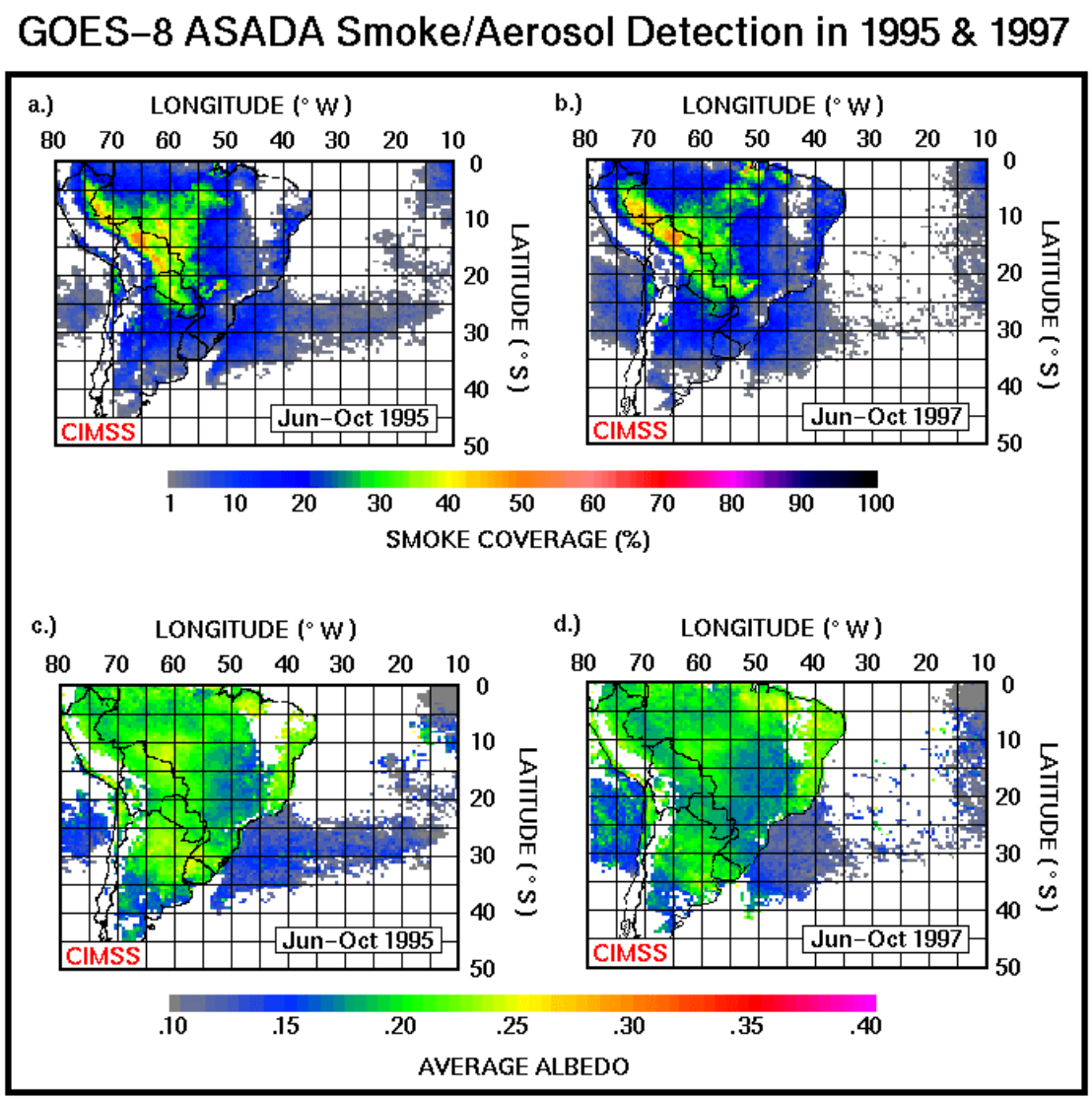

Figure 11. Composites a and b show the percentage of time a given area (on a .5 degree grid) was smoke covered at 11:45 UTC from June through October 1995 and 1997, respectively. Composites c and d show the average GOES-8 ASADA derived smoke albedo for the same time periods.